

SYSTEMATIC VARIATIONS IN THE WAVELENGTH DEPENDENCE OF INTERSTELLAR LINEAR POLARIZATION

D. C. B. WHITTET,^{1,2,3} P. G. MARTIN,¹ J. H. HOUGH,⁴ M. F. ROUSE,² J. A. BAILEY,^{5,6} AND D. J. AXON⁷

Received 1991 June 12; accepted 1991 August 21

ABSTRACT

This paper presents new observations of the wavelength dependence of interstellar linear polarization [$p(\lambda)$] made to investigate the influence of the environment on the effective size distribution of the aligned polarizing particles. Optical and infrared measurements were obtained simultaneously in eight photometric passbands between U and K , giving a coherent data set for a total of 105 reddened stars. The $p(\lambda)$ data were modeled using the usual Serkowski relation with three parameters: p_{\max} , λ_{\max} , and K . The added flexibility provided by the third parameter K offers a real improvement in fitting $p(\lambda)$ in the wavelength range 0.36–2.0 μm . Further modifications to the functional form of $p(\lambda)$ are necessary as the wavelength range is extended further.

We confirm that variations of K and λ_{\max} are correlated, and have revised slightly the empirical linear relationship between K and λ_{\max} found by Wilking et al. to $K = 0.01 \pm 0.05 + (1.66 \pm 0.09)\lambda_{\max}$. There is some cosmic scatter of the data about this line. A new finding is that the *same* linear dependence of K on λ_{\max} seen overall provides a consistent representation of the systematic polarization changes *within individual regions* with rather differing environments. Our qualitative explanation is that the grain size distribution in dense regions is modified by coagulation which removes the smaller particles without major modification of the larger ones. Alternatively, the size distribution in diffuse clouds is altered with respect to dense regions by the appearance of smaller particles, without major modification of the larger ones.

Subject headings: dust, extinction — ISM: general — polarization

1. INTRODUCTION

Variations in the spectral dependences of interstellar linear and circular polarization are of considerable significance to studies of interstellar grains, providing information on composition and growth and a potential means of distinguishing between alignment mechanisms (see Martin 1989 for a recent review). The observed linear polarization displays a broad peak in the optical region of the spectrum for most stars and can be described by the empirical formula (Serkowski 1973; Coyne, Gehrels, & Serkowski 1974; Serkowski, Mathewson, & Ford 1975)

$$p(\lambda)/p_{\max} = \exp[-K \ln^2(\lambda_{\max}/\lambda)], \quad (1)$$

where $p(\lambda)$ is the percentage polarization at wavelength λ and p_{\max} is the peak polarization, occurring at wavelength λ_{\max} . The parameter K , an inverse measure of the width of the polarization curve, was treated as a constant by Serkowski et al. (1975), who adopted a value of 1.15 for all stars. In this original form with $K = 1.15$, equation (1), the “Serkowski curve,” provides an adequate representation of the observations of interstellar polarization between wavelengths of 0.36 and 1.0 μm .

Codina-Landaberry & Magalhaes (1976) were first to suggest that the goodness of fit could be further improved by allowing K to vary. Extension of the wavelength coverage into the infrared showed discrepancies at wavelengths greater than 1 μm (Dyck & Jones 1978). Subsequently, Wilking et al. (1980, 1982) made more extensive infrared observations of stars with optical polarimetry available in the literature, giving a total spectral coverage of 0.35–2.2 μm for more than 30 lines of sight. They fitted the data using equation (1) with K treated as a third free parameter. They further deduced that the value of K for optimal fit to equation (1) increases linearly with λ_{\max} , according to the equation (Wilking et al. 1982)

$$K = (-0.10 \pm 0.05) + (1.86 \pm 0.09)\lambda_{\max}, \quad (2)$$

with λ_{\max} in microns.

The dependence of K on λ_{\max} reflects a decrease in the width of the polarization curve with increasing λ_{\max} ; in physical terms, this might be interpreted as a narrowing of the size distribution of the polarizing grains as the size (represented by λ_{\max}) increases, or as some systematic change in sphericity. The significance of the linear dependence summarized by equation (2) was questioned by Clarke & Al-Roubaie (1983), who argued that the form of the correlation between K and λ_{\max} depends on the number and choice of filter wavelengths in the data set. They suspected that the correlation might be due, at least in part, to random noise in the data, and suggested that any genuine astrophysical evidence for a relation between K and λ_{\max} can only be found by increasing the accuracy of the polarimetry.

The main purpose of this paper is to present new observations of the wavelength dependence of interstellar linear polarization made to address this issue. As described in § 2, optical and infrared measurements were obtained simultaneously in eight photometric passbands between U and K ,

¹ Canadian Institute for Theoretical Astrophysics, University of Toronto, 60 St George Street, Toronto, Ontario, Canada M5S 1A7.

² School of Physics and Astronomy, Lancashire Polytechnic, Preston PR1 2TQ, UK.

³ Postal address: Department of Physics, Rensselaer Polytechnic Institute, Troy, NY 12180.

⁴ Division of Physical Sciences, Hatfield Polytechnic, College Lane, Hatfield, Herts AL10 9AB, UK.

⁵ Anglo-Australian Observatory, PO Box 296, Epping, NSW 2121, Australia.

⁶ Postal address: Joint Astronomy Center, 665 Komohana Street, Hilo, HI 96720.

⁷ University of Manchester, Nuffield Radio Astronomy Laboratories, Jodrell Bank, Macclesfield, Cheshire SK11 9DL, UK.

giving a coherent data set for a total of 105 reddened stars. The size of the data set available to investigate the form of the polarization law is thus increased by a factor of more than 3. Compared to previous multiwavelength studies of interstellar polarization, the accuracy of our data is generally higher, with errors in $p(\lambda)$ frequently less than $\pm 0.1\%$ and in some cases less than $\pm 0.05\%$.

The data were modeled using three parameter fits based on equation (1) (§ 3). The results were then used to examine the significance of the proposed empirical linear relationship between K and λ_{\max} (§ 4). Evidence for regional variations in this relationship are sought in § 4.1. In § 5, we examine how the relationship might be used to illuminate the growth and alignment mechanisms for interstellar grains and to probe for any sensitivity to environment. Our conclusions are presented in § 6.

2. OBSERVATIONS

The observations were made during the course of several observing runs between 1985 February and 1987 February, with the Hatfield polarimeter on the 3.9 m Anglo-Australian Telescope (AAT) at Siding Spring Observatory, New South Wales, Australia, and the 3.8 m United Kingdom Infrared Telescope (UKIRT) at Mauna Kea Observatory, Hawaii. The construction and operation of the polarimeter are described by Brindle et al. (1986) and (in an earlier format) by Bailey & Hough (1982). For the observing runs of 1986 and 1987, the polarimeter was modified by the inclusion of a second optical channel, allowing simultaneous measurement in U or B (blue channel), and V , R , or I (red channel), in addition to J , H , or K (infrared channel). Bandpass characteristics are listed in Table 1: it should be noted, in particular, that our measurements at K are at an effective wavelength of $2.04 \mu\text{m}$, rather than the usual value of $2.2 \mu\text{m}$: absorption in the Foster prism both narrows the passband and reduces the effective wavelength.

Unpolarized standard stars were observed to check the instrumental polarization, which was found to be less than 0.03% in all the passbands. The polarization efficiency of the instrument was measured by the introduction of a Glan prism. This was found to be 100% in $UBVRI$ passbands, with some reduction in the infrared; all data presented below have been corrected for the latter. Position angles $\theta(\lambda)$ were calibrated by observations of interstellar polarization standards, selected from Serkowski et al. (1975).

Our data have been corrected for noise biasing using the analytical formula $p = p'[1 - (\sigma/p')^2]^{1/2}$ (Wardle & Kronberg 1974; Clarke & Stewart 1986), where σ is the standard deviation of the observed polarization p' . Because in general $\sigma \ll p'$ for our observations, the resulting corrections are small.

TABLE 1
PASSBAND CHARACTERISTICS

Filter	Central Wavelength (μm)	Half-Power Wavelengths (μm)
U	0.36	0.34–0.38
B	0.43	0.37–0.47
V	0.55	0.50–0.61
R	0.63	0.56–0.70
I	0.78	0.73–0.85
J	1.21	1.09–1.37
H	1.64	1.49–1.78
K	2.04	1.96–2.09

Our program stars were chosen to sample a variety of interstellar environments, including dense clouds, diffuse clouds, and low-density interstellar material. The stars observed are listed in Table 2, grouped according to location in the sky. Also given are celestial coordinates, visual magnitudes, spectral types and color excess, E_{B-V} , where available from the literature, with references in the final column.

The results of our polarimetric observations of $p(\lambda)$ and $\theta(\lambda)$ are given in Table 3 for each filter. The errors quoted are based on standard errors in the Stokes parameters, calculated from many individual integrations.

3. FITTING $p(\lambda)$

The three parameters K , p_{\max} and λ_{\max} of equation (1) were determined by a weighted nonlinear least-squares fit to the $p(\lambda)$ data for each star. The results for individual program stars are listed in Table 4; the errors are 1σ values formally determined during the fit. No fit was possible in the case of HD 147343, which has a low polarization and an erratic $p(\lambda)$. Results were also obtained for the same data but using $K = 1.15$ (the Serkowski form). Sample fits for three stars with contrasting values of λ_{\max} are shown in Figures 1a–1c (the vertical ranges are chosen such that the fits to the Serkowski form in each figure are just translated versions of the same curve).

Figure 1a illustrates that, as might be expected, there are some stars with intermediate values of λ_{\max} for which the two and three parameter fits are equally (un)satisfactory. Figure 1b shows a case in which both fits find a similar and longer λ_{\max} ; however, here the added flexibility provided by the third parameter allows the fit to be improved. Nevertheless, this illustrates a more general finding that the resulting values of p_{\max} and λ_{\max} are rather similar for the two fits, any differences usually being less than the formal errors, i.e., the form adopted for K is not usually critical to the evaluation of the particular parameters p_{\max} and λ_{\max} . Exceptions to this rule do occur for lower λ_{\max} , as discussed below.

Note that the three parameter curve in Figure 1b is narrower. This is an illustration of the systematic effect which can be summarized by a relationship like equation (2).

In Figure 1c we have results for a star whose polarization peaks in the blue. Here too the three parameter fit offers a significant improvement: the value of λ_{\max} is able to be smaller, and more realistic, and the fit to the polarization falloff in the near-infrared is achieved by a smaller value of K ; this systematic relationship between K and λ_{\max} is again like that of equation (2). By contrast, the two parameter curve is too narrow, and the fit can only be optimized by shifting λ_{\max} . Even in these poor fits, the parameter p_{\max} is fairly well determined.

Note that in this case, as opposed to the previous two with larger λ_{\max} , we have little or no information on the decay of $p(\lambda)$ for wavelengths shorter than λ_{\max} ; indeed for stars with polarization peaking far in the blue-ultraviolet, at the end of the range in which we have data, λ_{\max} is not necessarily well determined by fitting an equation like (1).

We conclude that the added flexibility provided by the third parameter K offers a real improvement in fitting $p(\lambda)$. Equation (1) provides an adequate description of the data, as judged by the χ^2 of the fits, in the wavelength range 0.36 – $2.0 \mu\text{m}$. However, there is no physics behind the *precise* (symmetrical log-normal) formulation of equation (1), and we cannot expect that the fitted $p(\lambda)$ curves can be extrapolated reliably further into the infrared or into the vacuum ultraviolet (Martin 1989). Indeed, the need for some modification is already suggested by

TABLE 2
PROGRAM STARS

Zone/Star	R.A. (1950)	Decl. (1950)	<i>V</i>	Spectral Type	<i>E_{B-V}</i>	Reference
NGC 1333 No. 3	03 ^b 26 ^m 04 ^s .8	+31°11'33"				19
No. 5	03 26 15.1	+31 08 03				19
Taurus Elias 1	04 15 34.6	+28 12 01		A5e		14
Elias 3	04 20 22.6	+24 53 13		K2 III	2.3:	14
Elias 9	04 29 09.6	+24 27 17		M4 III	1.3:	14
Elias 19	04 41 14.3	+25 19 20		M4 III	0.6:	14
Elias 29	04 34 12.0	+25 11 30		G9 III	0.9:	14
HD 28170	04 24 31.7	+24 57 03	8.95	A5 V	0.37	12
HD 28975	04 31 48.5	+24 08 30	9.02	A3	0.64:	13
HD 29333	04 35 17.1	+29 17 18	8.5:	A2		
HD 29647	04 38 03.7	+25 53 51	8.37	B6-7 IV	1.00	13, 18
HD 29835	04 40 00.4	+26 09 00	8.70	K2 III	0.32	12
HD 30168	04 43 07.5	+25 56 46	7.70	B8 V	0.46	12
HD 30675	04 47 44.0	+28 13 47	7.6:	B3		
HDE 279652	04 14 50.2	+37 35 54	9.82	A2 V	0.31	22
HDE 279658	04 13 47.3	+37 09 32	9.91	B7 V	0.67	22
HDE 283637	04 22 53.3	+27 30 18	11.27	B9	0.84:	13
HDE 283701	04 31 49.3	+27 06 03	9.66	A0 V	0.77	12
HDE 283725	04 35 58.9	+28 44 38	10.8:	F5		
HDE 283800	04 40 21.4	+26 56 03	9.78	B5 V	0.53	12
HDE 283809	04 38 20.7	+25 49 05	10.78	B3 V	1.61	17
HDE 283812	04 41 21.0	+25 26 13	9.54	A2 V	0.66	12
HDE 283855	04 45 06.5	+26 56 32	11.4:	A2		
M78 HD 38563A	05 44 09.5	+00 03 33	10.42	B3-5	0.78	1
HD 38563B	05 44 10.9	+00 04 17	10.56	B2 II-III	1.42	1
HD 38563C	05 44 11.5	+00 01 38	13.09	A0 II	0.96	1
CMa R1 No. 24	07 02 26.2	-10 51 41	13.31	A0 V	0.58	2
Vela I No. 81	09 00 30.6	-48 30 19	13.35	OB	1.32:	3
No. 95	09 04 16.2	-47 06 55	12.12	OB	1.95:	3
Cha DC F2	10 49 36.3	-77 42 13	9.90	B8 V	0.62	4
F3	10 49 49.2	-76 51 31	7.99	B2 V	0.70	4
F6	10 54 35.5	-76 35 47	11.06	A2 V	0.58	4
F7	10 54 56.3	-76 19 49	10.30	B5 V	0.58	4
F9	10 57 49.4	-76 49 49	9.58	K0 III	0.61	4
F11	10 59 52.9	-76 16 16	10.47	B9 V	0.80	4
F16	11 01 52.8	-77 04 52	11.49	G2 IV	0.81	4
F21	11 02 45.1	-76 35 59	11.41	K3 III	0.68	4
F27	11 05 33.2	-76 35 07				4
F28	11 05 51.6	-77 09 57	15.14	K4 III	1.10:	4
F29	11 06 31.1	-77 11 09	13.41	K4 III	0.31	4
F30	11 06 56.6	-76 32 15	11.44	K3 III	0.46	4
F32	11 08 13.6	-76 12 40	10.53	F0 V	0.39	4
F36	11 09 38.9	-77 15 10	13.76	K0 III	1.22	4
F40	11 13 42.8	-77 14 43	7.57	B8 III	0.65	4
T21	11 04 52.4	-77 05 41	11.25	G2	0.80:	4
T32	11 06 39.6	-77 23 01	8.46	B9.5 Ve	0.39	4
T41	11 08 17.9	-76 20 30	9.02	B9 V	0.43	4
Coalsack No. 48	12 36 10.1	-62 01 14	12.49	OB ⁺	1.9:	5
Cen OB No. 221	13 03 28.8	-62 35 50	12.73	OB	1.82:	6
No. 242	13 05 52.0	-62 11 31	11.96	O9.5 V	1.71	3, 6
Norma OBI-6	15 55 35.6	-53 48 47	11.60	O8 V	1.38	3
SLS 3318	15 08 57.6	-57 01 37	11.6:	OB ⁺		7
SLS 3386	15 38 22.4	-54 01 46	10.98	O6 If	1.94	3, 7
SLS 3401	15 44 48.9	-54 05 28	10.41	B1 II	0.97	3, 7
SLS 3404	15 45 36.4	-54 08 24	10.91	B1 IV	0.96	3, 7
SLS 3544	16 14 54.7	-51 20 35	12.1:	OB ⁺		7
ρ Oph Elias 14	16 23 01.7	-24 16 50				8
Elias 22	16 23 22.0	-24 14 15				8
Elias 25	16 23 32.8	-24 16 44	17.01	B3 V	2.90	8, 15
HD 147283	16 18 56.4	-24 22 40	10.27	A3 V	0.72	9
HD 147343	16 19 18.8	-24 14 47	9.36	A1 V	0.63	9
HD 147648	16 21 00.3	-25 17 59	9.42	B8 V	0.89	9
HD 150193	16 37 16.4	-23 47 56	8.81	A0e	0.54:	8, 10

TABLE 2—Continued

Zone/Star	R.A. (1950)	Decl. (1950)	V	Spectral Type	E_{B-V}	Reference
R CrA DC						
No. 2	18 58 31.8	-37 13 17	12.84	F7 III	0.45	11, 16
No. 10	18 59 48.8	-37 33 36	10.07	B8 V	0.69	11, 16
No. 12	19 01 27.7	-37 43 51	11.87	G8 III	0.53	11, 16
No. 13	19 01 58.8	-37 30 03	12.70	K1 III	0.33	11, 16
No. 15	19 01 49.5	-37 33 50	13.27	G1	0.2:	11, 16
No. 22	18 59 55.8	-36 57 57	11.50	K5 III	0.67	11, 16
No. 28	18 57 36.6	-36 46 00	10.54	M5 III	0.30:	11, 16
No. 30	18 58 41.4	-37 27 31	10.92	A0 V	0.58	11, 16
No. 43	18 54 58.4	-37 12 04	9.55	K0 III	0.46	11, 16
No. 46	18 56 40.0	-37 10 06	11.96	G8 III	0.54	11, 16
No. 50	18 55 26.0	-37 17 04	10.69	A6 V	0.33	11, 16
No. 52	18 55 11.1	-37 16 11	12.56	G5 III	0.46	11, 16
No. 56	19 03 01.7	-37 00 24	10.82	G5 IV	0.44	11, 16
No. 58	18 57 51.2	-37 30 20	11.47	K1 III	0.56	11, 16
No. 71	19 03 28.2	-37 13 19	12.13	F6 V	0.34	11, 16
No. 73	19 04 22.9	-37 17 48	12.38	G0 V	0.35	11, 16
No. 88	19 02 47.0	-37 22 48		G8		11
TY CrA ...	18 58 18.5	-36 56 51	9.10v	B9e	0.55:	10
Cyg OB2						
A	20 30 43.7	+41 03 53	13.12	OB	2.59	20
No. 3	20 29 49.9	+41 03 08	10.22	O9	1.93	20, 21
No. 4	20 30 26.3	+41 16 57	10.22	O7 III	1.49	20, 21
No. 5	20 30 34.8	+41 08 04	9.1v	O7f	2.00	20, 21
No. 6	20 30 58.0	+41 15 20	10.67	O8 V	1.54	20, 21
No. 7	20 31 26.5	+41 10 04	10.50	O3 If	1.77	20, 21
No. 8A	20 31 27.4	+41 08 33	8.98	O6 If	1.62	20, 21
No. 9	20 31 23.0	+41 04 51	10.80	O5 If	2.26	20, 21
No. 10	20 31 58.6	+41 22 39	9.88	O9.5 Ia	1.83	20, 21
No. 11	20 32 21.2	+41 26 39	10.04	O5 If	1.76	20, 21
No. 12	20 30 53.2	+41 04 14	11.47	B5 Ia ⁺	3.31	20, 21
No. 14	20 30 29.1	+41 15 21	11.61	OB	1.55	20
No. 15	20 30 40.1	+41 16 00	11.28	O8	1.51	20, 21
No. 17	20 31 28.1	+41 09 59	11.75	OB	1.68	20
No. 18	20 31 43.0	+41 05 05	11.09	OB	2.23	20
No. 19	20 31 51.5	+41 09 08	11.06	B0	1.92	20, 21
No. 21	20 30 40.1	+41 18 37	11.50	B1	1.34	20, 21
No. 22	20 31 21.1	+41 03 00	11.68	O5	2.33	20, 21
No. 24	20 31 29.7	+41 06 52	11.97	O7	1.92	20, 21
No. 25	20 31 38.3	+41 23 06	11.88	OB	1.60	20
NGC 7380 HD 215806	22 44 40.7	+58 01 53	9.15	B0 Ia	0.77	23
BD +57°2615	22 45 48.1	+57 52 47	10.24	B3	0.53	23
BD +57°2617	22 46 08.9	+57 46 35	10.2:	B8		
BD +57°22453	22 45 19.7	+57 53 53	10.8:	OB		

NOTE.—“v” denotes variable, whereas a colon denotes an uncertain value.

REFERENCES.—(1) Strom et al. 1975; (2) Herbst et al. 1978; (3) Bassino et al. 1982; (4) Whittet et al. 1987; (5) Muzzio & Orsatti 1977; (6) Muzzio 1979; (7) Stephenson & Sanduleak 1971; (8) Elias 1978a; (9) Whittet 1974; (10) Kilkeny et al. 1985; (11) Vrba et al. 1981; (12) Straižys & Meistas 1980; (13) Vrba & Rydgren 1985; (14) Elias 1978b; (15) Vrba et al. 1975; (16) Vrba & Rydgren 1984; (17) Straižys et al. 1985; (18) Crutcher 1985; (19) Strom et al. 1976; (20) Serkowski 1965; (21) Leitherer et al. 1982; (22) Ungerer et al. 1985; (23) Moffat 1971.

the near-infrared observations (Martin & Whittet 1990) and infrared observations at L and M by Nagata (1990), Jones (1990), and ourselves (Martin et al. 1992) bear this out.

4. CORRELATED CHANGES IN K AND λ_{\max}

Wilking et al. (1980, 1982) found that stars with shorter (longer) λ_{\max} had smaller (larger) values of K ; they found the linear relationship given in equation (2) and in line 2 of Table 5.

This systematic interdependence of K and λ_{\max} is confirmed in our data as well, as was illustrated in Figure 1. Figure 2 plots K versus λ_{\max} for all 104 stars in Table 4, and the trend can be seen clearly. A linear relationship is perhaps not the only one that might be considered, but is sufficient for the purposes here.

Systematic rotation of the electric vector with wavelength is generally indicative of the presence along the line of sight of two or more discrete interstellar clouds with individually dis-

tinct alignment properties and grain size distributions (Martin 1974), although it might also arise if the star is intrinsically polarized. In either case, the observed $p(\lambda)$ would be a composite. Thus Wilking et al. (1980, 1982) excluded these stars from their linear fit. In addition, Cyg OB2 A (VI Cyg A) has a polarization curve rising anomalously steeply to the blue, and lay furthest from the best straight line; it too was omitted from the fit. We adopted the same approach.

The position angle data for each star in Table 3 were examined to identify cases of wavelength dependence (electric vector rotation) significantly in excess of the typical errors in θ . A total of 25 such cases are identified by an asterisk in Table 4 (25% of the data set), as is Cyg OB2 A. These are marked with open circles in Figure 2 and are omitted from the determination of the best straight line. The line is a weighted least-squares fit to the data, with allowance for errors in

TABLE 3
OBSERVATIONS OF POLARIZATION AND POSITION ANGLE

Identification	λ	p	σ_p	θ	σ_θ	Identification	λ	p	σ_p	θ	σ_θ
NGC 1333 No. 3	<i>U</i>	0.96	0.11	100	3	HD 29333	<i>U</i>	4.49	0.17	72	1
	<i>B</i>	1.40	0.04	103	1		<i>B</i>	4.82	0.11	72	1
	<i>V</i>	2.08	0.03	110	1		<i>V</i>	5.31	0.06	71	1
	<i>R</i>	2.47	0.04	109	1		<i>R</i>	5.19	0.07	71	1
	<i>I</i>	2.84	0.05	111	1		<i>I</i>	4.75	0.09	71	1
	<i>J</i>	2.40	0.07	111	1		<i>J</i>	2.88	0.03	69	1
	<i>H</i>	1.65	0.05	112	5		<i>H</i>	1.81	0.04	68	1
	<i>K</i>	1.4	0.4	93	8		<i>K</i>	1.19	0.08	73	3
NGC 1333 No. 5	<i>U</i>	HD 29647	<i>U</i>	1.21	0.10	57	3
	<i>B</i>	3.5	0.9	118	2		<i>B</i>	1.67	0.06	64	2
	<i>V</i>	5.4	0.5	125	3		<i>V</i>	2.11	0.03	69	1
	<i>R</i>	7.00	0.10	132	1		<i>R</i>	2.25	0.05	72	1
	<i>I</i>	7.93	0.15	135	1		<i>I</i>	2.33	0.06	74	1
	<i>J</i>	6.81	0.02	142	1		<i>J</i>	1.70	0.02	78	1
	<i>H</i>	5.02	0.03	145	1		<i>H</i>	1.08	0.02	77	1
	<i>K</i>	3.41	0.04	149	1		<i>K</i>	0.73	0.06	80	2
Elias 1 (Taurus)	<i>U</i>	HD 29835	<i>U</i>	3.34	0.16	24	2
	<i>B</i>		<i>B</i>	4.04	0.05	24	2
	<i>V</i>	4.72	0.29	3	2		<i>V</i>	4.01	0.04	23	1
	<i>R</i>	5.28	0.03	2	1		<i>R</i>	3.92	0.07	22	1
	<i>I</i>	5.31	0.07	3	1		<i>I</i>	3.45	0.06	25	1
	<i>J</i>	4.30	0.04	1	1		<i>J</i>	1.82	0.05	23	1
	<i>H</i>	2.93	0.05	177	1		<i>H</i>	1.12	0.06	20	3
	<i>K</i>	2.16	0.13	176	2		<i>K</i>	0.87	0.07	14	8
Elias 3 (Taurus)	<i>U</i>	HD 30168	<i>U</i>	3.44	0.10	26	1
	<i>B</i>		<i>B</i>	4.01	0.15	25	1
	<i>V</i>		<i>V</i>	4.06	0.06	25	1
	<i>R</i>	2.80	0.22	97	1		<i>R</i>	4.06	0.04	24	1
	<i>I</i>	2.29	0.05	103	1		<i>I</i>	3.40	0.06	23	1
	<i>J</i>	1.79	0.03	109	1		<i>J</i>	2.17	0.05	25	1
	<i>H</i>	1.14	0.04	109	2		<i>H</i>	1.42	0.02	24	1
	<i>K</i>	0.76	0.06	113	2		<i>K</i>	0.74	0.08	28	6
Elias 9 (Taurus)	<i>U</i>	HD 30675	<i>U</i>	3.37	0.10	60	1
	<i>B</i>		<i>B</i>	3.70	0.12	58	1
	<i>V</i>		<i>V</i>	3.94	0.05	59	1
	<i>R</i>	0.32	0.09	175	8		<i>R</i>	3.72	0.08	57	1
	<i>I</i>	0.38	0.08	1	4		<i>I</i>	3.32	0.09	58	1
	<i>J</i>	0.44	0.02	145	3		<i>J</i>	1.90	0.09	58	1
	<i>H</i>	0.41	0.02	143	1		<i>H</i>	1.10	0.08	61	4
	<i>K</i>	0.22	0.02	146	5		<i>K</i>	0.74	0.12	62	7
Elias 19 (Taurus)	<i>U</i>	HDE 279652	<i>U</i>	1.20	0.20	91	3
	<i>B</i>	6.26	0.70	37	5		<i>B</i>	1.07	0.13	87	3
	<i>V</i>	6.20	0.17	38	1		<i>V</i>	1.29	0.06	90	1
	<i>R</i>	5.67	0.09	38	1		<i>R</i>	1.25	0.04	90	1
	<i>I</i>	5.22	0.06	36	1		<i>I</i>	1.03	0.05	86	1
	<i>J</i>	3.06	0.05	36	1		<i>J</i>	0.61	0.03	91	2
	<i>H</i>	1.94	0.03	35	1		<i>H</i>	0.45	0.04	93	3
	<i>K</i>	1.36	0.03	38	1		<i>K</i>
Elias 29 (Taurus)	<i>U</i>	HDE 279658	<i>U</i>	2.17	0.30	144	4
	<i>B</i>	4.50	0.20	44	9		<i>B</i>	2.68	0.02	147	1
	<i>V</i>	4.21	0.16	34	1		<i>V</i>	2.84	0.06	148	1
	<i>R</i>	4.34	0.11	31	1		<i>R</i>	2.76	0.05	146	1
	<i>I</i>	4.01	0.07	31	1		<i>I</i>	2.43	0.09	144	1
	<i>J</i>	2.43	0.02	29	1		<i>J</i>	1.42	0.03	147	1
	<i>H</i>	1.57	0.02	27	1		<i>H</i>	0.86	0.04	146	1
	<i>K</i>	1.07	0.10	34	4		<i>K</i>
HD 28170	<i>U</i>	1.60	0.04	90	2	HDE 283637	<i>U</i>
	<i>B</i>	1.79	0.08	90	1		<i>B</i>	2.40	0.09	7	1
	<i>V</i>	1.98	0.04	90	1		<i>V</i>	2.78	0.05	6	1
	<i>R</i>	1.92	0.04	88	1		<i>R</i>	2.68	0.07	6	1
	<i>I</i>	1.65	0.03	89	1		<i>I</i>	2.50	0.07	8	1
	<i>J</i>	1.03	0.02	89	1		<i>J</i>	1.57	0.05	6	1
	<i>H</i>	0.59	0.02	90	1		<i>H</i>	1.12	0.06	6	6
	<i>K</i>	0.49	0.12	87	10		<i>K</i>
HD 28975	<i>U</i>	2.73	0.03	56	4	HDE 283701	<i>U</i>	2.45	0.12	32	1
	<i>B</i>	3.11	0.06	56	1		<i>B</i>	2.93	0.08	33	1
	<i>V</i>	3.19	0.04	56	1		<i>V</i>	3.13	0.06	34	1
	<i>R</i>	3.11	0.06	56	1		<i>R</i>	3.18	0.06	31	1
	<i>I</i>	2.75	0.04	57	1		<i>I</i>	3.04	0.07	33	1
	<i>J</i>	1.77	0.05	60	1		<i>J</i>	1.68	0.12	42	5
	<i>H</i>	1.03	0.06	62	2		<i>H</i>	1.36	0.09	35	3
	<i>K</i>	0.87	0.12	39	6		<i>K</i>	0.86	0.08	23	8

TABLE 3—Continued

Identification	λ	p	σ_p	θ	σ_θ	Identification	λ	p	σ_p	θ	σ_θ
HDE 283725	<i>U</i>	4.37	0.07	68	1	Vel I No. 81	<i>U</i>	5.0	0.6	1	3
	<i>B</i>	4.77	0.05	68	1		<i>B</i>	6.1	0.3	1	1
	<i>V</i>	4.83	0.06	67	1		<i>V</i>	6.86	0.13	1	3
	<i>R</i>	4.76	0.09	66	1		<i>R</i>	6.85	0.19	1	1
	<i>I</i>	4.16	0.07	65	1		<i>I</i>	6.29	0.10	179	1
	<i>J</i>	2.50	0.03	66	1		<i>J</i>	3.65	0.03	5	1
	<i>H</i>	1.60	0.03	65	1		<i>H</i>	2.30	0.15	6	1
	<i>K</i>	1.23	0.09	69	5		<i>K</i>
HDE 283800	<i>U</i>	3.59	0.04	26	1	Vel I No. 95	<i>U</i>	6.05	0.50	172	3
	<i>B</i>	3.70	0.03	27	1		<i>B</i>	7.36	0.08	170	1
	<i>V</i>	4.06	0.09	27	1		<i>V</i>	8.21	0.05	168	1
	<i>R</i>	3.96	0.06	26	1		<i>R</i>	7.93	0.03	171	1
	<i>I</i>	3.58	0.07	27	1		<i>I</i>	7.08	0.03	171	1
	<i>J</i>	1.94	0.08	27	1		<i>J</i>	4.06	0.03	172	1
	<i>H</i>	1.36	0.06	29	2		<i>H</i>	2.32	0.05	169	1
	<i>K</i>		<i>K</i>	1.57	0.13	167	3
HDE 283809	<i>U</i>	Cha F2	<i>U</i>
	<i>B</i>	6.05	0.13	46	1		<i>B</i>	3.34	0.03	132	1
	<i>V</i>	6.63	0.07	49	1		<i>V</i>	3.78	0.03	136	1
	<i>R</i>	6.65	0.06	50	1		<i>R</i>	3.91	0.07	133	1
	<i>I</i>	6.27	0.03	52	1		<i>I</i>	3.59	0.10	133	1
	<i>J</i>	3.81	0.07	57	1		<i>J</i>	2.38	0.07	136	1
	<i>H</i>	2.59	0.07	58	1		<i>H</i>	1.43	0.08	132	2
	<i>K</i>	1.71	0.11	55	3		<i>K</i>
HDE 283812	<i>U</i>	5.16	0.11	32	1	Cha F3	<i>U</i>	3.51	0.10	121	1
	<i>B</i>	5.93	0.07	31	1		<i>B</i>	4.64	0.07	121	1
	<i>V</i>	6.29	0.05	32	1		<i>V</i>	5.20	0.08	121	1
	<i>R</i>	6.29	0.07	31	1		<i>R</i>	5.38	0.07	122	1
	<i>I</i>	5.68	0.07	31	1		<i>I</i>	5.11	0.12	123	1
	<i>J</i>	3.21	0.06	32	1		<i>J</i>	3.50	0.08	123	1
	<i>H</i>	2.09	0.04	31	1		<i>H</i>	1.98	0.05	124	1
	<i>K</i>	1.31	0.07	35	2		<i>K</i>	1.17	0.06	122	2
HDE 283855	<i>U</i>	4.57	0.05	46	1	Cha F6	<i>U</i>	4.66	0.33	122	2
	<i>B</i>	4.90	0.06	46	1		<i>B</i>	4.98	0.06	119	1
	<i>V</i>	5.28	0.07	46	1		<i>V</i>	5.51	0.04	118	1
	<i>R</i>	4.92	0.07	45	1		<i>R</i>	5.40	0.05	118	1
	<i>I</i>	4.37	0.08	46	1		<i>I</i>	4.97	0.07	117	1
	<i>J</i>	2.58	0.03	46	1		<i>J</i>	3.02	0.05	116	1
	<i>H</i>	1.67	0.06	47	3		<i>H</i>	1.81	0.04	116	1
	<i>K</i>		<i>K</i>	1.95	0.70	127	10
HD 38563A	<i>U</i>	2.88	0.08	96	1	Cha F7	<i>U</i>	4.98	0.17	118	1
	<i>B</i>	3.64	0.03	95	1		<i>B</i>	5.64	0.03	118	1
	<i>V</i>	4.19	0.05	97	2		<i>V</i>	5.98	0.05	118	1
	<i>R</i>	4.47	0.05	96	1		<i>R</i>	5.91	0.05	118	1
	<i>I</i>	4.22	0.03	99	1		<i>I</i>	5.39	0.07	117	1
	<i>J</i>	2.58	0.05	100	2		<i>J</i>	3.19	0.05	118	1
	<i>H</i>	1.57	0.05	97	1		<i>H</i>	1.92	0.03	118	2
	<i>K</i>	0.61	0.06	93	5		<i>K</i>	1.19	0.01	126	4
HD 38563B	<i>U</i>	Cha F9	<i>U</i>	3.52	0.33	126	3
	<i>B</i>	1.00	0.17	174	5		<i>B</i>	4.21	0.03	126	1
	<i>V</i>	1.78	0.12	4	3		<i>V</i>	4.68	0.10	128	1
	<i>R</i>	2.28	0.06	5	2		<i>R</i>	4.89	0.08	126	1
	<i>I</i>	2.57	0.07	8	1		<i>I</i>	4.66	0.09	126	1
	<i>J</i>	1.85	0.05	11	1		<i>J</i>	3.09	0.06	130	1
	<i>H</i>	1.20	0.08	15	2		<i>H</i>	1.92	0.05	130	1
	<i>K</i>	0.59	0.16	12	9		<i>K</i>	1.26	0.06	126	2
HD 38563C	<i>U</i>	Cha F11	<i>U</i>
	<i>B</i>	7.76	0.42	73	1		<i>B</i>	4.60	0.05	111	1
	<i>V</i>	8.73	0.24	73	1		<i>V</i>	4.97	0.14	111	1
	<i>R</i>	9.17	0.25	73	1		<i>R</i>	4.83	0.10	110	5
	<i>I</i>	8.96	0.26	72	1		<i>I</i>	4.16	0.05	106	4
	<i>J</i>	6.03	0.10	71	1		<i>J</i>	2.27	0.09	108	1
	<i>H</i>	3.68	0.10	70	1		<i>H</i>	1.53	0.06	111	2
	<i>K</i>	2.21	0.55	78	17		<i>K</i>	0.79	0.10	113	4
CMa R1 No. 24	<i>U</i>	Cha F16	<i>U</i>
	<i>B</i>	3.16	0.10	89	3		<i>B</i>	6.19	0.16	117	1
	<i>V</i>	3.67	0.18	84	2		<i>V</i>	7.09	0.11	119	1
	<i>R</i>	3.18	0.09	86	1		<i>R</i>	7.32	0.10	120	1
	<i>I</i>	3.24	0.10	89	1		<i>I</i>	6.87	0.15	120	1
	<i>J</i>	2.10	0.05	86	1		<i>J</i>	4.26	0.11	122	1
	<i>H</i>	1.43	0.10	88	3		<i>H</i>	2.62	0.06	123	1
	<i>K</i>		<i>K</i>	1.53	0.07	118	5

TABLE 3—Continued

Identification	λ	p	σ_p	θ	σ_θ	Identification	λ	p	σ_p	θ	σ_θ
Cha F21	<i>U</i>	Cha T32	<i>U</i>
	<i>B</i>	5.27	0.19	118	1		<i>B</i>	2.26	0.05	141	1
	<i>V</i>	5.37	0.09	118	1		<i>V</i>	2.57	0.08	143	1
	<i>R</i>	4.98	0.07	117	1		<i>R</i>	2.76	0.06	142	1
	<i>I</i>	4.51	0.07	116	1		<i>I</i>	2.53	0.05	143	1
	<i>J</i>	2.64	0.06	116	1		<i>J</i>	1.54	0.07	141	2
	<i>H</i>	1.63	0.05	117	1		<i>H</i>	0.84	0.03	129	1
<i>K</i>	1.10	0.07	114	2	<i>K</i>	0.67	0.05	121	4		
Cha F27	<i>U</i>	Cha T41	<i>U</i>
	<i>B</i>	5.7	0.3	119	1		<i>B</i>	2.41	0.19	130	2
	<i>V</i>	5.80	0.14	119	1		<i>V</i>	2.87	0.06	132	2
	<i>R</i>	6.09	0.10	118	1		<i>R</i>	3.03	0.12	130	2
	<i>I</i>	5.76	0.07	115	1		<i>I</i>	3.22	0.08	132	1
	<i>J</i>	3.37	0.03	118	1		<i>J</i>	2.13	0.05	133	2
	<i>H</i>	2.00	0.05	118	1		<i>H</i>	1.27	0.12	133	1
<i>K</i>	1.28	0.16	116	5	<i>K</i>		
Cha F28	<i>U</i>	Coalsack No. 48	<i>U</i>
	<i>B</i>	5.6	0.9	136	12		<i>B</i>	5.28	0.10	98	1
	<i>V</i>	6.4	0.4	139	2		<i>V</i>	5.81	0.09	98	1
	<i>R</i>	6.6	0.3	134	2		<i>R</i>	5.54	0.09	97	1
	<i>I</i>	7.09	0.10	134	1		<i>I</i>	4.93	0.10	98	1
	<i>J</i>	4.94	0.04	140	1		<i>J</i>	2.43	0.06	100	1
	<i>H</i>	3.15	0.07	142	1		<i>H</i>	1.61	0.05	101	1
<i>K</i>	2.14	0.11	135	2	<i>K</i>	1.21	0.10	102	2		
Cha F29	<i>U</i>	Cen OB No. 221	<i>U</i>
	<i>B</i>	4.39	0.21	150	2		<i>B</i>	3.11	0.23	79	2
	<i>V</i>	4.89	0.19	149	1		<i>V</i>	3.59	0.07	77	1
	<i>R</i>	5.01	0.06	149	1		<i>R</i>	3.52	0.09	76	1
	<i>I</i>	4.94	0.06	149	1		<i>I</i>	3.16	0.07	76	1
	<i>J</i>	3.38	0.01	150	1		<i>J</i>	1.81	0.05	78	1
	<i>H</i>	2.29	0.10	149	4		<i>H</i>	1.09	0.04	79	1
<i>K</i>	<i>K</i>	0.67	0.09	88	9		
Cha F30	<i>U</i>	Cen OB No. 242	<i>U</i>
	<i>B</i>	4.14	0.05	110	1		<i>B</i>	3.28	0.11	73	2
	<i>V</i>	4.59	0.16	107	1		<i>V</i>	3.40	0.06	73	1
	<i>R</i>	4.36	0.16	106	1		<i>R</i>	3.33	0.08	72	1
	<i>I</i>	4.13	0.14	103	1		<i>I</i>	2.85	0.05	72	1
	<i>J</i>	2.64	0.12	100	2		<i>J</i>	1.54	0.07	71	1
	<i>H</i>	1.70	0.05	100	1		<i>H</i>	0.80	0.07	70	3
<i>K</i>	1.07	0.05	95	1	<i>K</i>	0.58	0.08	69	3		
Cha F32	<i>U</i>	Nor OB I-6	<i>U</i>
	<i>B</i>	2.21	0.03	109	1		<i>B</i>	2.27	0.11	64	1
	<i>V</i>	2.32	0.09	108	1		<i>V</i>	2.47	0.07	64	1
	<i>R</i>	2.31	0.02	107	1		<i>R</i>	2.41	0.06	65	1
	<i>I</i>	2.26	0.14	108	1		<i>I</i>	2.06	0.05	65	1
	<i>J</i>	1.36	0.06	108	1		<i>J</i>	1.22	0.05	68	1
	<i>H</i>	0.94	0.09	109	2		<i>H</i>	0.76	0.05	66	2
<i>K</i>	0.51	0.08	102	4	<i>K</i>	0.78	0.21	67	21		
Cha F36	<i>U</i>	SLS 3318	<i>U</i>
	<i>B</i>	10.3	0.7	134	2		<i>B</i>	8.82	0.10	61	1
	<i>V</i>	11.49	0.15	134	1		<i>V</i>	9.53	0.19	63	1
	<i>R</i>	12.26	0.13	134	1		<i>R</i>	9.64	0.17	61	1
	<i>I</i>	12.00	0.10	134	1		<i>I</i>	8.30	0.15	60	1
	<i>J</i>	7.95	0.03	133	1		<i>J</i>	5.11	0.11	63	1
	<i>H</i>	5.05	0.04	133	1		<i>H</i>	3.19	0.08	60	1
<i>K</i>	2.79	0.07	135	1	<i>K</i>	2.21	0.08	57	1		
Cha F40	<i>U</i>	6.15	0.17	132	1	SLS 3386	<i>U</i>	4.61	0.45	81	2
	<i>B</i>	7.39	0.06	131	1		<i>B</i>	5.18	0.08	78	1
	<i>V</i>	8.03	0.04	133	1		<i>V</i>	5.15	0.06	76	1
	<i>R</i>	8.04	0.04	130	1		<i>R</i>	5.19	0.03	77	1
	<i>I</i>	7.10	0.05	130	1		<i>I</i>	4.59	0.06	74	1
	<i>J</i>	4.46	0.07	132	1		<i>J</i>	2.76	0.02	71	1
	<i>H</i>	2.67	0.04	131	1		<i>H</i>	1.58	0.04	70	1
<i>K</i>	1.91	0.11	122	2	<i>K</i>	1.29	0.08	65	3		
Cha T21	<i>U</i>	SLS 3401	<i>U</i>	3.36	0.13	47	1
	<i>B</i>	2.49	0.16	134	2		<i>B</i>	3.97	0.06	46	1
	<i>V</i>	2.90	0.09	135	1		<i>V</i>	4.37	0.08	45	1
	<i>R</i>	3.09	0.16	138	2		<i>R</i>	4.32	0.06	45	1
	<i>I</i>	3.29	0.17	139	1		<i>I</i>	3.85	0.07	45	1
	<i>J</i>	1.75	0.17	145	3		<i>J</i>	2.23	0.06	45	1
	<i>H</i>	1.22	0.05	146	2		<i>H</i>	1.33	0.05	41	1
<i>K</i>	0.79	0.05	150	5	<i>K</i>	1.15	0.05	46	2		

TABLE 3—Continued

Identification	λ	p	σ_p	θ	σ_θ	Identification	λ	p	σ_p	θ	σ_θ
SLS 3404	<i>U</i>	3.77	0.15	49	1	R CrA No. 2	<i>U</i>
	<i>B</i>	4.48	0.05	48	1		<i>B</i>	0.83	0.23	22	8
	<i>V</i>	4.82	0.05	48	1		<i>V</i>	1.40	0.09	10	2
	<i>R</i>	4.75	0.05	48	1		<i>R</i>	1.48	0.09	11	2
	<i>I</i>	4.21	0.05	48	1		<i>I</i>	1.96	0.10	7	1
	<i>J</i>	2.43	0.07	48	1		<i>J</i>	1.54	0.03	8	1
	<i>H</i>	1.48	0.03	47	1		<i>H</i>	1.09	0.02	9	1
	<i>K</i>	0.91	0.18	44	6		<i>K</i>	1.13	0.15	171	8
SLS 3544	<i>U</i>	7.77	0.22	56	1	R CrA No. 10	<i>U</i>
	<i>B</i>	8.71	0.08	55	1		<i>B</i>	0.45	0.04	160	2
	<i>V</i>	8.50	0.07	55	1		<i>V</i>	0.51	0.03	168	2
	<i>R</i>	7.93	0.06	55	1		<i>R</i>	0.66	0.05	162	2
	<i>I</i>	6.42	0.07	55	1		<i>I</i>	0.63	0.04	167	2
	<i>J</i>	3.25	0.04	56	1		<i>J</i>	0.60	0.05	172	2
	<i>H</i>	1.82	0.03	55	1		<i>H</i>	0.39	0.05	172	4
	<i>K</i>	1.15	0.07	55	1		<i>K</i>	0.30	0.08	140	16
Elias 14 (ρ Oph)	<i>U</i>	R CrA No. 12	<i>U</i>
	<i>B</i>		<i>B</i>	0.50	0.09	133	5
	<i>V</i>	5.77	0.21	177	1		<i>V</i>	0.76	0.04	129	2
	<i>R</i>	6.17	0.17	1	1		<i>R</i>	0.79	0.05	129	1
	<i>I</i>	6.67	0.07	2	1		<i>I</i>	0.76	0.05	126	2
	<i>J</i>	4.95	0.02	2	1		<i>J</i>	0.66	0.04	127	2
	<i>H</i>	3.24	0.03	3	1		<i>H</i>	0.40	0.04	131	3
	<i>K</i>	1.95	0.03	3	1		<i>K</i>	0.28	0.13	141	13
Elias 22 (ρ Oph)	<i>U</i>	R CrA No. 13	<i>U</i>
	<i>B</i>	3.2	0.7	5	5		<i>B</i>	1.8	0.3	100	4
	<i>V</i>	3.93	0.30	0	2		<i>V</i>	2.25	0.09	102	1
	<i>R</i>	5.02	0.14	0	1		<i>R</i>	2.45	0.08	99	1
	<i>I</i>	5.25	0.07	178	1		<i>I</i>	2.71	0.07	97	1
	<i>J</i>	3.79	0.02	176	1		<i>J</i>	2.21	0.03	96	1
	<i>H</i>	2.21	0.03	177	1		<i>H</i>	1.40	0.03	94	1
	<i>K</i>	0.99	0.05	1	2		<i>K</i>	0.86	0.15	102	5
Elias 25 (ρ Oph)	<i>U</i>	R CrA No. 15	<i>U</i>
	<i>B</i>		<i>B</i>	2.18	0.18	101	2
	<i>V</i>	8.4	1.6	22	5		<i>V</i>	2.56	0.10	100	1
	<i>R</i>		<i>R</i>	2.73	0.09	97	1
	<i>I</i>	8.96	0.09	23	1		<i>I</i>	3.18	0.09	96	1
	<i>J</i>	6.46	0.02	24	1		<i>J</i>	2.28	0.03	96	1
	<i>H</i>	4.13	0.02	24	1		<i>H</i>	1.44	0.06	100	2
	<i>K</i>		<i>K</i>
HD 147283	<i>U</i>	R CrA No. 22	<i>U</i>
	<i>B</i>	1.01	0.06	175	1		<i>B</i>	1.42	0.31	87	2
	<i>V</i>	1.34	0.05	175	2		<i>V</i>	1.22	0.08	92	4
	<i>R</i>	1.59	0.03	174	1		<i>R</i>	1.17	0.08	82	2
	<i>I</i>	1.62	0.07	174	1		<i>I</i>	1.04	0.07	84	2
	<i>J</i>	1.17	0.03	173	1		<i>J</i>	0.48	0.02	83	3
	<i>H</i>	0.91	0.05	172	2		<i>H</i>	0.29	0.05	80	5
	<i>K</i>	0.48	0.04	171	7		<i>K</i>
HD 147343	<i>U</i>	R CrA No. 28	<i>U</i>
	<i>B</i>	0.41	0.06	163	4		<i>B</i>	1.47	0.09	56	1
	<i>V</i>	0.41	0.06	163	4		<i>V</i>	1.79	0.04	58	1
	<i>R</i>	0.43	0.05	151	3		<i>R</i>	2.01	0.05	56	1
	<i>I</i>	0.24	0.08	140	7		<i>I</i>	2.10	0.04	52	1
	<i>J</i>	0.22	0.03	128	4		<i>J</i>	1.71	0.06	57	1
	<i>H</i>	0.45	0.06	87	4		<i>H</i>	1.00	0.04	58	2
	<i>K</i>	0.33	0.10	137	7		<i>K</i>	0.75	0.05	53	2
HD 147648	<i>U</i>	1.11	0.10	26	3	R CrA No. 30	<i>U</i>
	<i>B</i>	1.10	0.04	31	1		<i>B</i>	1.22	0.05	138	1
	<i>V</i>	1.11	0.04	34	1		<i>V</i>	1.58	0.05	139	1
	<i>R</i>	0.89	0.04	41	1		<i>R</i>	1.71	0.04	139	1
	<i>I</i>	0.75	0.04	41	1		<i>I</i>	1.89	0.04	137	1
	<i>J</i>	0.36	0.03	43	3		<i>J</i>	1.48	0.03	137	1
	<i>H</i>	0.32	0.03	40	3		<i>H</i>	1.03	0.03	139	1
	<i>K</i>	0.17	0.01	40	9		<i>K</i>	0.29	0.13	167	12
HD 150193	<i>U</i>	3.19	0.15	57	1	R CrA No. 43	<i>U</i>	1.00	0.10	71	3
	<i>B</i>	4.32	0.07	56	1		<i>B</i>	1.45	0.04	68	1
	<i>V</i>	5.08	0.04	56	1		<i>V</i>	1.47	0.05	69	1
	<i>R</i>	5.19	0.05	56	1		<i>R</i>	1.76	0.05	66	1
	<i>I</i>	4.99	0.06	57	1		<i>I</i>	1.73	0.05	66	1
	<i>J</i>	3.27	0.06	57	1		<i>J</i>	1.30	0.03	70	1
	<i>H</i>	2.26	0.03	60	1		<i>H</i>	0.96	0.04	70	2
	<i>K</i>	1.68	0.02	60	1		<i>K</i>	0.47	0.06	62	4

TABLE 3—Continued

Identification	λ	p	σ_p	θ	σ_θ	Identification	λ	p	σ_p	θ	σ_θ
R CrA No. 46	<i>U</i>	Cyg OB2 A	<i>U</i>
	<i>B</i>	1.55	0.10	35	2		<i>B</i>	7.6	0.7	117	1
	<i>V</i>	2.06	0.07	36	1		<i>V</i>	6.63	0.16	119	1
	<i>R</i>	2.43	0.06	31	1		<i>R</i>	5.91	0.06	118	1
	<i>I</i>	2.78	0.07	33	1		<i>I</i>	4.57	0.07	118	1
	<i>J</i>	2.18	0.05	33	1		<i>J</i>	1.85	0.08	119	1
	<i>H</i>	1.37	0.04	32	1		<i>H</i>	0.81	0.04	121	1
	<i>K</i>	0.87	0.04	29	3		<i>K</i>	0.53	0.06	126	4
R CrA No. 50	<i>U</i>	Cyg OB2 No. 3	<i>U</i>	5.07	0.16	106	1
	<i>B</i>	0.76	0.04	33	2		<i>B</i>	5.43	0.05	106	1
	<i>V</i>	1.01	0.04	32	1		<i>V</i>	5.51	0.07	107	1
	<i>R</i>	1.13	0.05	32	2		<i>R</i>	5.29	0.04	106	1
	<i>I</i>	1.05	0.04	33	1		<i>I</i>	4.60	0.06	106	1
	<i>J</i>	0.91	0.04	32	1		<i>J</i>	2.80	0.03	105	1
	<i>H</i>	0.52	0.05	29	3		<i>H</i>	1.81	0.03	105	1
	<i>K</i>		<i>K</i>	1.15	0.04	108	1
R CrA No. 52	<i>U</i>	Cyg OB2 No. 4	<i>U</i>	2.17	0.11	77	2
	<i>B</i>	1.53	0.13	32	5		<i>B</i>	2.16	0.05	73	1
	<i>V</i>	1.83	0.10	40	1		<i>V</i>	2.09	0.06	77	1
	<i>R</i>	2.01	0.07	40	1		<i>R</i>	2.07	0.05	75	1
	<i>I</i>	1.99	0.08	39	1		<i>I</i>	1.63	0.05	75	1
	<i>J</i>	1.38	0.04	39	1		<i>J</i>	0.92	0.03	81	2
	<i>H</i>	0.84	0.02	38	1		<i>H</i>	0.55	0.03	79	3
	<i>K</i>	0.69	0.07	51	4		<i>K</i>	0.33	0.07	52	10
R CrA No. 56	<i>U</i>	Cyg OB2 No. 5	<i>U</i>	3.63	0.07	87	1
	<i>B</i>	1.76	0.08	68	1		<i>B</i>	3.63	0.05	85	1
	<i>V</i>	1.93	0.06	69	1		<i>V</i>	3.75	0.05	84	1
	<i>R</i>	2.21	0.06	67	1		<i>R</i>	3.53	0.04	84	1
	<i>I</i>	1.98	0.03	70	1		<i>I</i>	3.17	0.03	82	1
	<i>J</i>	1.41	0.04	70	1		<i>J</i>	2.04	0.04	85	1
	<i>H</i>	0.81	0.02	70	1		<i>H</i>	1.38	0.02	86	1
	<i>K</i>	0.50	0.10	77	6		<i>K</i>	1.03	0.02	92	2
R CrA No. 58	<i>U</i>	Cyg OB2 No. 6	<i>U</i>	1.54	0.04	56	1
	<i>B</i>	0.68	0.04	0	4		<i>B</i>	1.67	0.06	57	2
	<i>V</i>	0.74	0.13	174	6		<i>V</i>	1.68	0.06	53	1
	<i>R</i>	0.82	0.12	172	3		<i>R</i>	1.65	0.04	52	1
	<i>I</i>	0.75	0.06	176	2		<i>I</i>	1.31	0.03	50	1
	<i>J</i>	0.58	0.04	178	2		<i>J</i>	0.78	0.02	52	1
	<i>H</i>	0.30	0.09	173	7		<i>H</i>	0.42	0.03	46	4
	<i>K</i>		<i>K</i>	0.13	0.09	37	21
R CrA No. 71	<i>U</i>	0.71	0.10	50	4	Cyg OB2 No. 7	<i>U</i>	3.32	0.12	95	1
	<i>B</i>	0.76	0.09	51	4		<i>B</i>	3.52	0.07	96	1
	<i>V</i>	0.94	0.08	48	3		<i>V</i>	3.67	0.05	96	1
	<i>R</i>	0.98	0.10	51	3		<i>R</i>	3.48	0.04	95	1
	<i>I</i>	1.04	0.08	50	2		<i>I</i>	3.02	0.03	95	1
	<i>J</i>	0.74	0.05	52	2		<i>J</i>	1.77	0.02	96	1
	<i>H</i>	0.39	0.06	63	7		<i>H</i>	1.14	0.02	95	1
	<i>K</i>		<i>K</i>	0.76	0.04	98	2
R CrA No. 73	<i>U</i>	Cyg OB2 No. 8A	<i>U</i>	1.08	0.07	84	1
	<i>B</i>	1.50	0.10	84	2		<i>B</i>	1.18	0.04	84	1
	<i>V</i>	1.71	0.07	83	2		<i>V</i>	1.34	0.04	83	1
	<i>R</i>	1.82	0.07	86	1		<i>R</i>	1.32	0.04	80	1
	<i>I</i>	1.80	0.07	86	1		<i>I</i>	1.20	0.04	79	2
	<i>J</i>	1.16	0.05	84	1		<i>J</i>	0.78	0.02	81	1
	<i>H</i>	0.75	0.01	86	1		<i>H</i>	0.46	0.02	82	2
	<i>K</i>		<i>K</i>	0.30	0.03	79	1
R CrA No. 88	<i>U</i>	Cyg OB2 No. 9	<i>U</i>	2.79	0.21	52	1
	<i>B</i>	2.87	0.13	84	2		<i>B</i>	2.65	0.05	52	1
	<i>V</i>	3.92	0.10	86	1		<i>V</i>	2.61	0.05	51	1
	<i>R</i>	4.20	0.12	86	1		<i>R</i>	2.53	0.04	47	1
	<i>I</i>	4.86	0.13	87	1		<i>I</i>	2.21	0.04	47	1
	<i>J</i>	3.87	0.06	90	1		<i>J</i>	1.34	0.04	45	1
	<i>H</i>	2.73	0.07	92	1		<i>H</i>	0.81	0.04	44	2
	<i>K</i>	1.84	0.09	95	1		<i>K</i>	0.58	0.04	51	3
TY CrA	<i>U</i>	0.42	0.10	108	7	Cyg OB2 No. 10	<i>U</i>	0.60	0.13	47	4
	<i>B</i>	0.72	0.05	100	2		<i>B</i>	0.66	0.06	53	3
	<i>V</i>	0.85	0.03	98	1		<i>V</i>	0.59	0.06	50	2
	<i>R</i>	0.76	0.05	100	2		<i>R</i>	0.50	0.02	50	3
	<i>I</i>	0.74	0.06	94	2		<i>I</i>	0.39	0.04	47	4
	<i>J</i>	0.43	0.07	89	3		<i>J</i>	0.15	0.04	50	2
	<i>H</i>	0.41	0.05	106	3		<i>H</i>	0.13	0.03	34	8
	<i>K</i>	0.26	0.03	104	4		<i>K</i>

TABLE 3—Continued

Identification	λ	p	σ_p	θ	σ_θ	Identification	λ	p	σ_p	θ	σ_θ
Cyg OB2 No. 11	<i>U</i>	2.92	0.15	161	1	Cyg OB2 No. 22	<i>U</i>	1.50	0.04	173	5
	<i>B</i>	2.98	0.07	161	1		<i>B</i>	1.50	0.09	175	3
	<i>V</i>	3.16	0.05	160	1		<i>V</i>	1.74	0.04	179	1
	<i>R</i>	3.15	0.03	159	1		<i>R</i>	1.73	0.07	178	1
	<i>I</i>	2.78	0.03	159	1		<i>I</i>	1.58	0.05	0	1
	<i>J</i>	1.75	0.02	160	1		<i>J</i>	1.02	0.02	2	1
	<i>H</i>	1.13	0.02	157	1		<i>H</i>	0.66	0.02	2	1
<i>K</i>	0.79	0.04	160	2	<i>K</i>	0.42	0.04	7	2		
Cyg OB2 No. 12	<i>U</i>	Cyg OB2 No. 24	<i>U</i>
	<i>B</i>	9.67	0.10	119	1		<i>B</i>	2.08	0.10	61	1
	<i>V</i>	8.72	0.11	119	1		<i>V</i>	2.48	0.08	62	1
	<i>R</i>	7.97	0.05	117	1		<i>R</i>	2.32	0.10	62	1
	<i>I</i>	7.06	0.05	117	1		<i>I</i>	2.13	0.05	62	1
	<i>J</i>	3.90	0.04	116	1		<i>J</i>	1.36	0.03	63	1
	<i>H</i>	2.35	0.02	115	1		<i>H</i>	0.89	0.03	65	2
<i>K</i>	1.65	0.02	118	1	<i>K</i>	0.43	0.16	84	13		
Cyg OB2 No. 14	<i>U</i>	3.15	0.06	89	1	Cyg OB2 No. 25	<i>U</i>	4.0	0.5	62	2
	<i>B</i>	3.20	0.10	86	1		<i>B</i>	4.12	0.11	66	1
	<i>V</i>	3.29	0.06	87	1		<i>V</i>	4.01	0.06	65	1
	<i>R</i>	3.13	0.05	86	1		<i>R</i>	3.70	0.04	65	1
	<i>I</i>	2.63	0.04	88	1		<i>I</i>	3.11	0.04	65	1
	<i>J</i>	1.54	0.02	88	1		<i>J</i>	1.71	0.04	66	1
	<i>H</i>	0.96	0.03	87	1		<i>H</i>	1.10	0.02	64	1
<i>K</i>	<i>K</i>	0.55	0.10	78	7		
Cyg OB2 No. 15	<i>U</i>	2.90	0.05	86	1	HD 215806	<i>U</i>	1.55	0.09	68	1
	<i>B</i>	3.13	0.09	87	1		<i>B</i>	1.87	0.04	66	1
	<i>V</i>	3.19	0.05	86	1		<i>V</i>	1.84	0.05	67	1
	<i>R</i>	2.98	0.04	85	1		<i>R</i>	1.83	0.04	66	1
	<i>I</i>	2.61	0.06	85	1		<i>I</i>	1.53	0.05	67	1
	<i>J</i>	1.43	0.06	85	1		<i>J</i>	0.77	0.06	75	3
	<i>H</i>	0.96	0.03	87	1		<i>H</i>	0.58	0.05	79	3
<i>K</i>	0.74	0.25	85	3	<i>K</i>	0.55	0.06	77	12		
Cyg OB2 No. 17	<i>U</i>	BD + 57°2615	<i>U</i>	1.82	0.05	45	2
	<i>B</i>	3.84	0.18	97	1		<i>B</i>	1.91	0.07	42	1
	<i>V</i>	4.11	0.12	99	1		<i>V</i>	2.00	0.04	42	1
	<i>R</i>	4.10	0.09	98	1		<i>R</i>	2.02	0.05	41	1
	<i>I</i>	3.36	0.07	97	1		<i>I</i>	1.71	0.05	41	1
	<i>J</i>	2.02	0.04	98	1		<i>J</i>	0.73	0.10	30	3
	<i>H</i>	1.28	0.03	98	1		<i>H</i>	0.72	0.06	26	3
<i>K</i>	<i>K</i>		
Cyg OB2 No. 18	<i>U</i>	1.05	0.35	90	10	BD + 57°2617	<i>U</i>	0.88	0.05	63	4
	<i>B</i>	1.20	0.09	109	2		<i>B</i>	1.00	0.06	58	2
	<i>V</i>	1.49	0.04	108	1		<i>V</i>	1.10	0.07	59	1
	<i>R</i>	1.51	0.04	107	1		<i>R</i>	1.06	0.04	58	1
	<i>I</i>	1.43	0.05	106	1		<i>I</i>	0.83	0.07	59	3
	<i>J</i>	1.00	0.02	105	1		<i>J</i>	0.51	0.03	60	1
	<i>H</i>	0.66	0.05	104	2		<i>H</i>	0.26	0.06	41	7
<i>K</i>	0.41	0.05	108	4	<i>K</i>		
Cyg OB2 No. 19	<i>U</i>	1.85	0.35	91	1	BD + 57°22453	<i>U</i>
	<i>B</i>	2.02	0.08	91	1		<i>B</i>	1.72	0.11	68	1
	<i>V</i>	2.43	0.05	95	1		<i>V</i>	1.75	0.07	69	1
	<i>R</i>	2.41	0.03	95	1		<i>R</i>	1.62	0.09	71	2
	<i>I</i>	2.33	0.04	95	1		<i>I</i>	1.39	0.08	70	2
	<i>J</i>	1.55	0.02	95	1		<i>J</i>	0.73	0.07	71	3
	<i>H</i>	0.98	0.02	96	1		<i>H</i>
<i>K</i>	0.57	0.04	104	3	<i>K</i>		
Cyg OB2 No. 21	<i>U</i>	3.19	0.16	57	1						
	<i>B</i>	3.44	0.07	56	1						
	<i>V</i>	3.40	0.06	56	1						
	<i>R</i>	3.22	0.04	55	1						
	<i>I</i>	2.69	0.07	54	1						
	<i>J</i>	1.74	0.05	55	1						
	<i>H</i>	1.28	0.08	56	2						
<i>K</i>							

TABLE 4
FITTED VALUES OF p_{\max} , λ_{\max} , AND K

Identification	p_{\max}	σ	λ_{\max}	σ	K	σ
NGC 1333 No. 3	2.86	0.03	0.88	0.01	1.43	0.05*
No. 5	7.73	0.10	0.86	0.02	1.07	0.06*
Elias 1 (Taurus)	5.39	0.04	0.73	0.02	0.93	0.07*
Elias 3 (Taurus)	2.36	0.15	0.72	0.11	1.03	0.34*
Elias 9 (Taurus)	0.46	0.06	1.15	0.18	1.89	1.17*
Elias 19 (Taurus)	6.58	0.61	0.41	0.07	0.62	0.12
Elias 29 (Taurus)	4.59	0.25	0.46	0.05	0.68	0.10*
HD 28170	1.92	0.03	0.55	0.01	0.98	0.06
HD 28975	3.17	0.03	0.54	0.01	0.89	0.05
HD 29333	5.25	0.07	0.54	0.02	0.89	0.07
HD 29647	2.30	0.02	0.73	0.01	1.15	0.04*
HD 29835	4.07	0.07	0.50	0.03	0.93	0.11
HD 30168	4.07	0.09	0.53	0.03	0.83	0.09
HD 30675	3.90	0.03	0.52	0.01	0.99	0.05
HDE 279652	1.29	0.09	0.47	0.09	0.78	0.26
HDE 279658	2.81	0.03	0.53	0.01	0.99	0.06
HDE 283637	2.72	0.07	0.57	0.05	0.89	0.19
HDE 283701	3.18	0.04	0.60	0.02	0.89	0.07
HDE 283725	4.84	0.07	0.50	0.02	0.79	0.06
HDE 283800	3.92	0.11	0.53	0.02	0.86	0.14
HDE 283809	6.70	0.10	0.59	0.02	0.97	0.10*
HDE 283812	6.30	0.09	0.55	0.02	0.96	0.07
HDE 283855	5.13	0.09	0.51	0.01	0.91	0.07
M78 HD 38563A	4.43	0.06	0.64	0.01	1.28	0.07
HD 38563B	2.53	0.09	0.82	0.02	1.81	0.26*
HD 38563C	9.14	0.07	0.65	0.01	1.07	0.04
CMa R1 No. 24	3.36	0.12	0.56	0.05	0.78	0.19
Vel I No. 81	6.89	0.12	0.58	0.02	1.17	0.12
No. 95	8.08	0.07	0.55	0.01	1.10	0.06
Cha F2	3.85	0.02	0.62	0.01	1.06	0.04
Cha F3	5.40	0.07	0.64	0.01	1.14	0.05
Cha F6	5.47	0.04	0.57	0.01	1.01	0.05
Cha F7	5.97	0.04	0.55	0.01	0.94	0.02
Cha F9	4.84	0.04	0.63	0.01	0.99	0.03
Cha F11	4.82	0.08	0.53	0.02	0.96	0.10
Cha F16	7.24	0.08	0.62	0.01	1.09	0.06*
Cha F21	5.41	0.14	0.47	0.03	0.76	0.08
Cha F27	6.13	0.18	0.58	0.04	1.09	0.15
Cha F28	7.09	0.19	0.67	0.04	1.01	0.12
Cha F29	5.05	0.08	0.64	0.03	0.97	0.13
Cha F30	4.46	0.05	0.57	0.01	0.88	0.04*
Cha F32	2.34	0.02	0.56	0.01	0.87	0.05
Cha F36	12.15	0.30	0.64	0.03	1.04	0.11
Cha F40	8.02	0.07	0.57	0.01	0.99	0.06
Cha T21	3.07	0.13	0.67	0.04	1.12	0.17*
Cha R32	2.68	0.08	0.62	0.02	1.19	0.12*
Cha T41	3.18	0.07	0.71	0.02	1.39	0.16
Coalsack No. 48	5.67	0.24	0.52	0.05	1.00	0.22
Cen OB No. 221	3.58	0.07	0.54	0.03	0.98	0.11
No. 242	3.42	0.05	0.51	0.02	1.05	0.08
Nor OB I-6	2.45	0.07	0.51	0.04	0.89	0.14
SLS 3318	9.37	0.19	0.54	0.02	0.88	0.09
SLS 3386	5.32	0.09	0.52	0.02	0.90	0.09*
SLS 3401	4.32	0.07	0.57	0.01	1.07	0.08
SLS 3404	4.79	0.04	0.55	0.01	1.01	0.04
SLS 3544	8.76	0.18	0.45	0.02	0.95	0.07
Elias 14 (ρ Oph)	6.56	0.16	0.74	0.03	1.17	0.09*
Elias 22 (ρ Oph)	5.23	0.14	0.77	0.03	1.59	0.15
Elias 25 (ρ Oph)	9.18	0.08	0.66	0.01	0.98	0.02
HD 147283	1.61	0.07	0.76	0.03	1.24	0.22
HD 147343	0.00	0.00	0.00	0.00	0.00	0.00*
HD 147648	1.19	0.15	0.32	0.09	0.57	0.16*
HD 150193	5.10	0.13	0.64	0.04	0.86	0.10
R CrA No. 2	1.78	0.07	0.87	0.03	1.23	0.19*
No. 10	0.65	0.04	0.84	0.04	0.97	0.23*
No. 12	0.81	0.03	0.75	0.03	1.11	0.22

INTERSTELLAR LINEAR POLARIZATION

TABLE 4—Continued

Identification	P_{\max}	σ	λ_{\max}	σ	K	σ
No. 13	2.72	0.03	0.81	0.01	1.34	0.06*
No. 15	3.00	0.11	0.77	0.03	1.29	0.22
No. 22	1.30	0.15	0.46	0.11	1.05	0.39
No. 28	2.10	0.05	0.77	0.02	1.20	0.12
No. 30	1.85	0.05	0.79	0.02	1.16	0.14
No. 43	1.73	0.08	0.71	0.03	0.93	0.16
No. 46	2.71	0.05	0.83	0.01	1.42	0.08
No. 50	1.11	0.05	0.76	0.03	1.15	0.22
No. 52	1.99	0.06	0.68	0.04	1.11	0.15
No. 56	2.08	0.04	0.65	0.03	1.09	0.11
No. 58	0.80	0.03	0.65	0.03	0.92	0.19
No. 71	1.03	0.04	0.69	0.02	1.17	0.16
No. 73	1.80	0.04	0.65	0.03	1.04	0.11
No. 88	4.65	0.08	0.82	0.01	1.13	0.07*
Ty CrA	0.81	0.04	0.62	0.07	0.84	0.23*
Cyg OB2 A	7.60	0.58	0.39	0.04	1.06	0.12*
No. 3	5.53	0.07	0.48	0.02	0.76	0.05
No. 4	2.20	0.05	0.44	0.03	0.83	0.08
No. 5	3.73	0.06	0.46	0.02	0.60	0.04
No. 6	1.69	0.03	0.49	0.02	0.95	0.08*
No. 7	3.66	0.09	0.47	0.03	0.77	0.08
No. 8	1.32	0.01	0.58	0.01	0.97	0.04
No. 9	2.69	0.03	0.46	0.02	0.73	0.05*
No. 10	0.69	0.10	0.33	0.08	0.74	0.24
No. 11	3.19	0.06	0.51	0.03	0.78	0.07
No. 12	9.90	0.67	0.35	0.05	0.60	0.08
No. 14	3.32	0.06	0.46	0.02	0.80	0.06
No. 15	3.16	0.04	0.49	0.02	0.83	0.06
No. 17	4.18	0.23	0.46	0.06	0.76	0.14
No. 18	1.50	0.02	0.64	0.02	0.98	0.07
No. 19	2.42	0.02	0.63	0.01	1.00	0.06
No. 21	3.46	0.09	0.44	0.04	0.66	0.10
No. 22	1.72	0.03	0.55	0.01	0.82	0.05*
No. 24	2.35	0.07	0.55	0.04	0.86	0.13
No. 25	4.28	0.19	0.39	0.04	0.68	0.08
NGC 7380 HD 215806	1.87	0.06	0.49	0.05	0.82	0.19
BD + 57°2615	2.02	0.06	0.51	0.03	0.88	0.18*
BD + 57°2617	1.07	0.02	0.54	0.02	1.16	0.11
BD + 57°22453	1.76	0.02	0.49	0.02	1.07	0.09

NOTE.—Asterisks (*) denote stars excluded from fits of K vs. λ_{\max} .

both variables. The parameters of this fit are listed in Table 5, line 5. Line 3 removes HD 38463B from the Wilking et al. (1980, 1982) data set, since we found for it electric vector rotation. For completeness, Table 5 also lists results without this selection for rotation (lines 1 and 4); they are not dramatically different.

The fits to selected stars (lines 3 and 5) are similar within the formal errors, and so the data were combined for a final assessment (109 stars). The best fit, given in line 6 of Table 5 and appearing in Figures 2–5, is

$$K = 0.01 \pm 0.05 + (1.66 \pm 0.09)\lambda_{\max} \quad (3)$$

This is consistent with equation (2) (or lines 2 and 3 in Table 5 or the original fit in Wilking et al. 1980). Despite the much larger data set, the formal errors of the slope and intercept have not decreased significantly. This points to there being “cosmic scatter” in the fitted parameters of the polarization curves that exceeds their formal errors.

Cosmic scatter can be examined by means of Figure 3, where we show the combined (selected) data. The stars have been divided into four equal groups according to the formal quality of the parameters K and λ_{\max} as fitted in equation (1). There is not a large reduction in the scatter of the points about the best line as the quality is increased (*small points, plus signs, squares,*

and open circles). Nor is the fit to the best quarter of the points (errors less than ± 0.057 in K and $\pm 0.034 \mu\text{m}$ in λ_{\max}) significantly different, or better (line 7 of Table 5). The presence of cosmic scatter suggests that an unweighted linear fit be considered. This is given in line 8 of Table 5, and is again not significantly different (it is also like the geometric mean of the two unweighted linear regressions). Thus the linear dependence found is rather robust. A conservative summary which encompasses the above fits and the regional analyses below is $K = 1.7\lambda_{\max}$ (line 14 of Table 5).

4.1. Regional Variations

A remarkable uniformity in the behavior of the polarization law (in different interstellar environments—see § 5) is illustrated by the continuity of the data in Figures 2 and 3. We have substantial subsets of data in five individual regions, namely Taurus, Chamaeleon I, ρ Oph, R CrA and Cyg OB2. These subsets have different mean values of λ_{\max} . It is therefore interesting to ask whether the overall linear relationship found is the result of combining regions with characteristically different λ_{\max} and K , or whether it is present within a single region.

Figure 4 illustrates the K versus λ_{\max} behavior for Cyg OB2 coupled with R CrA, essentially juxtaposing the behavior in diffuse cloud and dense cloud environments. Because λ_{\max} and

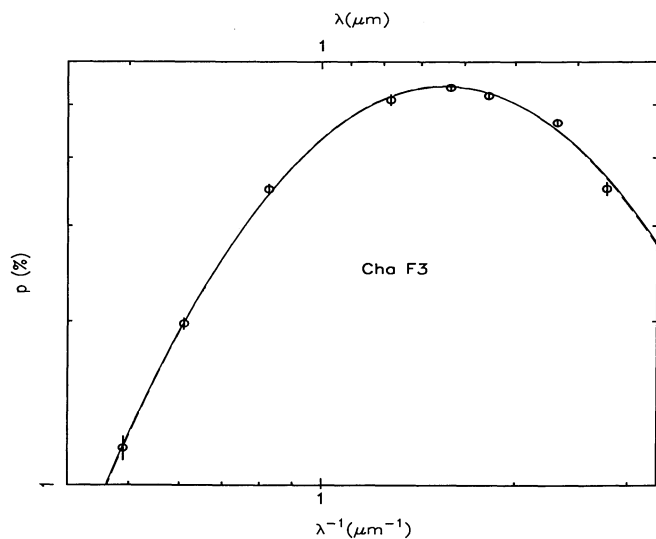


FIG. 1a

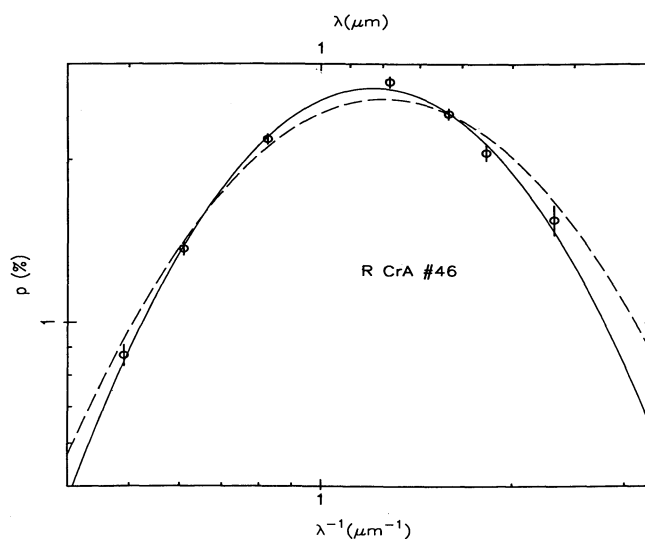


FIG. 1b

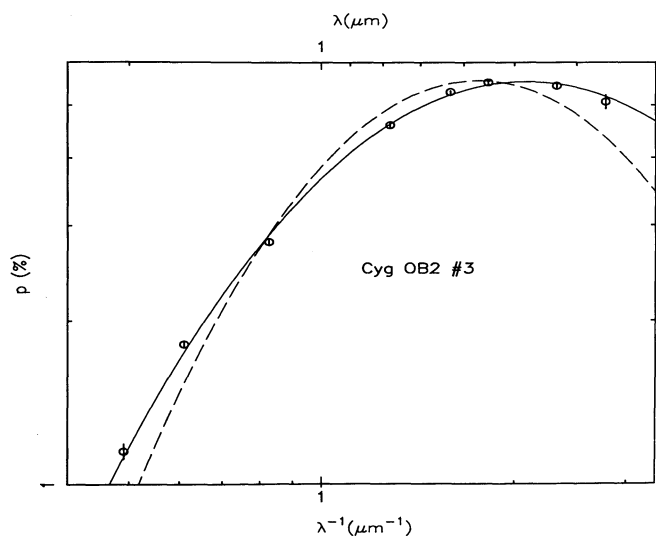


FIG. 1c

FIG. 1.—Sample fits of $p(\lambda)$ for contrasting values of λ_{\max} . The dashed curve, from a two parameter fit to equation (1) with $K = 1.15$, is the same (within a translation) in each of these log-log plots. (a) Cha F3, with $\lambda_{\max} = 0.64$, is equally well modeled using a two or three parameter fit. (b) R CrA No. 46 has a narrower polarization curve, better modeled by a more flexible three parameter fit, in which K and λ_{\max} are both lower, following equation (2). (c) Cyg OB2 No. 3 has a broader polarization curve (smaller K), and smaller λ_{\max} . The two parameter fit is inadequate.

K tend to be higher in R CrA than in Cyg OB2, there is little overlap of the data sets for the two regions. Superposed is the best straight line found above from all of the regions (eq. [3]). It is clear that the individual regions Cyg OB2 and R CrA are consistent with the overall average. More significantly, *within each individual region* the same qualitative dependence of K on λ_{\max} is apparent. The formal fits for the two individual regions are in Table 5, lines 13 and 12, respectively.

As a further example, Figure 5 shows the corresponding plot for Taurus and ρ Oph (this paper; Wilking et al. 1980, 1982). Again there is little overlap of the data sets in the diagram, and a consistency of each region with the general trend (lines 9 and

11 in Table 5, respectively). The Chamaeleon region (not plotted) also fits into this general picture, having intermediate values of K and λ_{\max} and a similar slope (line 10). Of the five regions examined, ρ Oph presents the strongest impression of having different (steeper) linear dependence; however, this possibility is not of high statistical significance (line 11) and needs to be investigated further.

5. SYSTEMATIC VARIATIONS, SIZE DISTRIBUTIONS, AND ALIGNMENT

Clearly, the interdependence of λ_{\max} and the width of the polarization curve (or K) distills important information about the way in which grains evolve and are aligned. We have seen in § 4.1 that the *same* linear dependence of K on λ_{\max} found overall provides a reasonable representation *within* different regions. In this section we wish to emphasize that these are diverse regions which have different densities, different levels of

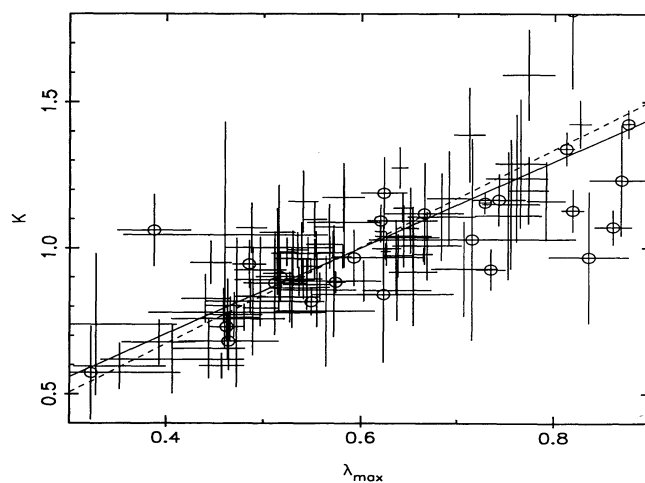


FIG. 2.— K vs. λ_{\max} for all 104 stars in Table 4. The open symbols identify stars for which there is a significant rotation of the electric vector with wavelength and Cyg OB2 A (those marked by an asterisk in Table 4). These stars are omitted in finding the best straight line shown (line 5 in Table 5). Also shown as a dashed line is the best fit adopted from combination of our selected data with that of Wilking et al. (1980, 1982; Fig. 3 and line 6 of Table 5).

TABLE 5
LINEAR RELATIONSHIP BETWEEN K AND λ_{\max}

Data Set Selection	Size	Intercept	Slope	Quality ^a
1 (Wilking et al. 1980, 1982)	37	-0.08 ± 0.07	1.85 ± 0.13	1.84
2 (no rotation)	32	-0.10 ± 0.05	1.86 ± 0.10	0.90
3 (less HD 38563B)	31	-0.07 ± 0.05	1.80 ± 0.09	0.81
4 (Table 4, this paper)	104	0.19 ± 0.06	1.33 ± 0.09	1.86
5 (no rotation)	78	0.12 ± 0.08	1.47 ± 0.14	1.60
6 (combine 3 and 5)	109	0.01 ± 0.05	1.66 ± 0.09	1.41
7 ("best" quarter)	27	-0.04 ± 0.09	1.72 ± 0.16	2.41
8 (unweighted)	109	-0.06 ± 0.06	1.79 ± 0.10	...
9 (Taurus)	15	0.11 ± 0.13	1.52 ± 0.63	0.87
10 (Cha)	14	0.08 ± 0.20	1.55 ± 0.35	1.09
11 (ρ Oph)	11	-0.97 ± 0.42	3.00 ± 0.60	1.50
12 (R CrA)	13	-0.20 ± 0.30	1.87 ± 0.40	0.46
13 (Cyg OB2)	16	-0.04 ± 0.12	1.70 ± 0.24	0.84
14 (conservative summary)	0.0 ± 0.1	1.7 ± 0.2	...

^a χ^2 per degree of freedom.

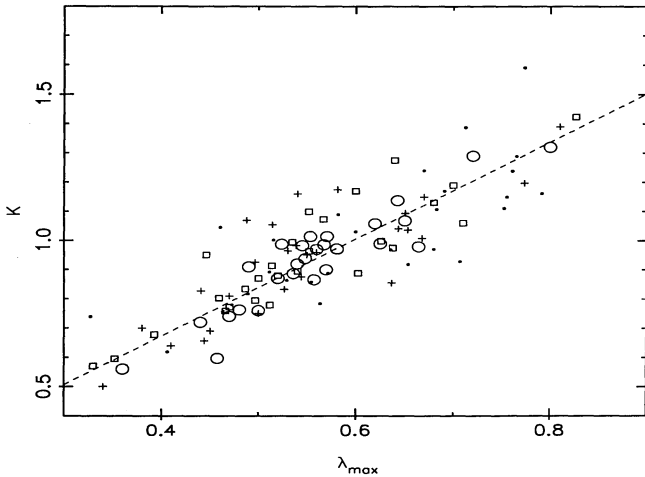


FIG. 3.— K vs. λ_{\max} for our selected stars and those of Wilking et al. (1980, 1982). The linear fit shown is also line 6 of Table 5. In lieu of error bars, the stars have been divided into four equal groups according to the formal quality of the determination of K and λ_{\max} . As the quality is increased (*small points, plus signs, squares, and open circles*), the scatter of the points about the best line is not dramatically reduced.

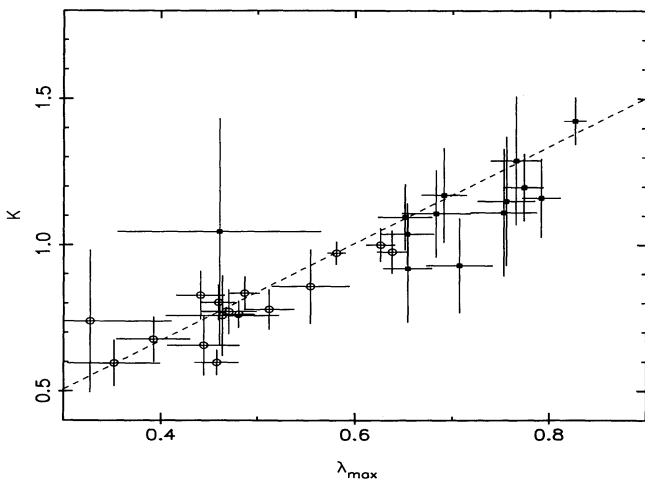


FIG. 4.— K vs. λ_{\max} for Cyg OB2 (*open circles*) and R CrA (*filled squares*). The interdependence of K and λ_{\max} can be seen within each individual region, and is consistent with the dashed line, the overall relation for all regions (line 6 of Table 5).

star-formation activity, and potentially different mechanisms for modifying the grain distribution.

Grain alignment in the interstellar medium is with respect to the Galactic magnetic field. Hildebrand (1988) reviewed various alignment mechanisms and observational constraints and concluded that the alignment is of superparamagnetic grains by the Davis & Greenstein (1951) mechanism. It is well-known that λ_{\max} is generally higher in dense clouds than in regions of lower density (e.g., Carrasco, Strom, & Strom 1973; Vrba, Coyne, & Tapia 1981), and that λ_{\max} shows a distinct correlation with the ratio of total to selective extinction (e.g., Serkowski et al. 1975; Whittet & van Breda 1978; Clayton & Mathis 1988). The present results confirm this general picture, the highest λ_{\max} values occurring in nearby molecular clouds such as R CrA and ρ Oph (Figs. 4 and 5). Detailed discussion and analysis, based on the current data set, of variations in λ_{\max} with variations in the extinction curve, the dependence of p_{\max} on the amount of extinction, and the spatial distribution within individual dark clouds is left for future investigation.

In the line of sight to the Cygnus OB2 association, the observed reddening occurs predominantly in diffuse foreground material (Adamson, Whittet, & Duley 1990, and references therein). The low values of λ_{\max} are assumed to indicate

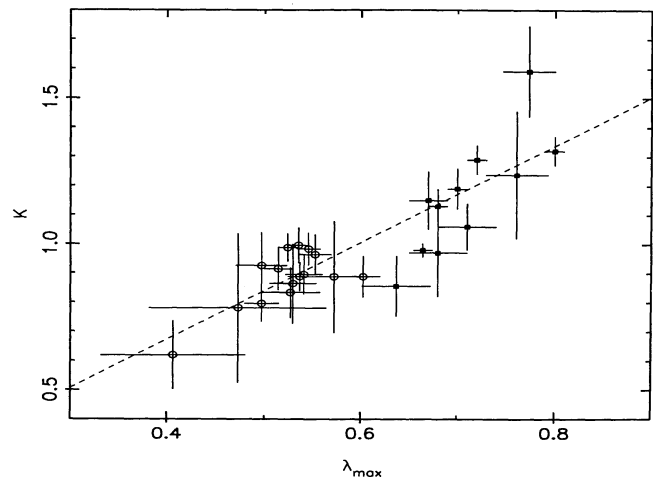


FIG. 5.—Like Fig. 4, but for Taurus (*open circles*), and ρ Oph (*filled squares*).

an absence of processing of the grains in a manner which enhances the average size, as typically tends to occur in denser environments; or since grains cycle between the diffuse and molecular cloud environments, one might say alternatively that the low values of λ_{\max} indicate that the grains have undergone a decrease in average size since their last sojourn in a denser environment.

The other selected regions are dark clouds with varying degrees of apparent star-formation activity. Taurus is comparatively quiescent, lacking massive young stars (e.g., Elias 1978b), and is hence devoid of large-scale shocks and hard ultraviolet radiation fields associated with embedded OB stars. The environment in the Taurus cloud is conducive to the growth and survival of icy grain mantles, as demonstrated observationally by Whittet et al. (1988, 1989), and we note that two stars in our current sample (HD 29647 and HD 283809) have evidence for water-ice absorption at $3.05 \mu\text{m}$. In Taurus λ_{\max} has not increased very much.

In contrast, the ρ Oph dark cloud contains an emergent OB association (Wilking & Lada 1983), the least obscured members of which illuminate prominent reflection nebulae. Grain growth in this region has been significant and is generally associated with grain coagulation (Jura 1980); accretion of molecular ice mantles from the gas occurs only at $A_V > 10$ (Tanaka et al. 1990). In terms of star formation activity, Chamaeleon I and R CrA appear to be intermediate cases (see Table 2 for references).

The environment clearly affects $p(\lambda)$, changing λ_{\max} and K systematically from place to place. The evolution of the size distribution of the grains from the diffuse interstellar medium through dark clouds and regions of star formation might involve a variety of physical processes, including size-dependent accretion, coagulation, and selective small-grain destruction, some or all of which might occur to different degrees in our sample. However, to within the limits of the available data, regions with demonstrably different environments obey the same general form of the polarization law. We therefore conclude that the environment does not impose any further strikingly unique characteristics on the particular linear dependence of K on λ_{\max} shown in equation (3).

On the assumption that increases in λ_{\max} are produced by grain growth resulting from ice mantle accretion, Aannestad & Greenberg (1983) calculated the dependence of the width of $p(\lambda)$ on λ_{\max} . They concluded that a model with suprathreshold alignment provides a good fit to observational data from Wilking et al. (1980). However, as Mathis (1986) pointed out, this is not really the case, and our own data confirm that none of their accretion models succeeds in reproducing the trend. From this, and the above discussion of the different regions, we conclude specifically that ice mantle growth is not relevant to causing major changes in λ_{\max} . Nor is it expected to be, since the observed ice band optical depths can be explained by relatively thin ice mantles (Whittet et al. 1988).

Major changes in λ_{\max} might be consistent with coagulation. From a study which showed an invariance of the slope of infrared polarization with changes in λ_{\max} , in addition to an invariance of infrared extinction with changes in the ratio of total to selective extinction, Martin & Whittet (1990) concluded that removal of the smaller particles, perhaps by coagulation with larger particles, is a possible explanation. In this view the larger particles do not grow significantly (say by mutual coagulation). The narrowing of the $p(\lambda)$ curve with increasing λ_{\max} , the additional effect being discussed here,

would be interpreted naturally as a narrowing of the size distribution of the aligned grains as the smaller particles are removed.

Any interpretation should also take into account the potential effects of changes in alignment efficiency with grain size. A potential problem with (thermal) magnetic alignment is a tendency for an increasing degree of disalignment as the grains grow larger, ultimately leading to an increase in the width of $p(\lambda)$ (decrease of K) with λ_{\max} , contrary to observations. This might not be a problem for our interpretation in which the larger grains are already aligned and do not grow substantially, or if perfect spinning alignment were achieved for all particles. In any case, to counteract this—to maintain the smaller widths seen at longer λ_{\max} —one could assume that the magnetic enhancement factors are consistently greater for larger grains. This might arise if grains are magnetized by small superparamagnetic inclusions as discussed by Mathis (1986); in this model, alignment occurs only if at least one such inclusion is present, with a probability proportional to volume. Mathis has also suggested that the probability of two grains coagulating might depend on whether or not they already contain superparamagnetic inclusions. All of this presents the possibility of more subtle scenarios for the evolution of the effective size distribution of *aligned polarizing* particles, beyond that seen for all of the particles causing extinction. However, the evidence is that extinction and polarization are rather similarly affected by changes in the environment (Martin & Whittet 1990).

6. CONCLUSIONS

The added flexibility provided by the third parameter K in equation (1) offers a real improvement in fitting $p(\lambda)$ in the wavelength range $0.36\text{--}2.0 \mu\text{m}$. Further modifications to the functional form of $p(\lambda)$ are necessary as the wavelength range is extended further (Martin et al. 1992).

We confirm the linear relationship between the fitted parameters K and λ_{\max} , and find evidence for cosmic scatter about it. Our best fit (eq. [3]; line 6 of Table 5) is $K = 0.01 \pm 0.05 + (1.66 \pm 0.09)\lambda_{\max}$.

The *same* linear dependence of K on λ_{\max} seen overall provides an adequate representation of the systematic changes in the polarization curves of stars *within individual regions* which have different densities, different amounts of ice accretion, and different levels of star-formation activity. A consistent qualitative explanation is that the grain size distribution in dense regions is modified by coagulation which removes the smaller particles without major modification of the larger ones. Alternatively, the size distribution in diffuse clouds is altered with respect to dense regions by the appearance of smaller particles, without major modification of the larger ones; this has interesting implications for the reverse process, destruction of interstellar grains.

We are grateful to the Science and Engineering Research Council (SERC) and the Natural Sciences and Engineering Research Council of Canada for financial support. P. G. M. acknowledges further research support from the Connaught Fund of the University of Toronto. M. F. R. acknowledges receipt of an SERC Research Studentship. Observing time was awarded by the SERC Panel for the Allocation of Telescope Time. The United Kingdom Infrared Telescope is operated by the Royal Observatory, Edinburgh, on behalf of the SERC.

REFERENCES

- Aannestad, P. A., & Greenberg, J. M. 1983, *ApJ*, 272, 551
 Adamson, A. J., Whittet, D. C. B., & Duley, W. W. 1990, *MNRAS*, 243, 400
 Bailey, J. A., & Hough, J. H. 1982, *PASP*, 94, 618
 Bassino, L. P., Dessauet, V. H., Muzzio, J. C., & Waldhausen, S. 1982, *MNRAS*, 201, 885
 Brindle, C., Hough, J. H., Bailey, J. A., Axon, D. J., & Hyland, A. R. 1986, *MNRAS*, 221, 739
 Carrasco, L., Strom, S. E., & Strom, K. M. 1973, *ApJ*, 182, 95
 Clarke, D., & Al-Roubaie, A. 1983, *MNRAS*, 202, 173
 Clarke, D., & Stewart, B. G. 1986, *Vistas Astron.*, 29, 27
 Clayton, G. C., & Mathis, J. S. 1988, *ApJ*, 327, 911
 Codina-Landaberry, S., & Magalhaes, A. M. 1976, *A&A*, 49, 407
 Coyne, G. V., Gehrels, T., & Serkowski, K. 1974, *AJ*, 79, 581
 Crutcher, R. M. 1985, *ApJ*, 288, 604
 Davis, L., & Greenstein, J. L. 1951, *ApJ*, 114, 206
 Dyck, H. M., & Jones, T. J. 1978, *AJ*, 83, 594
 Elias, J. H. 1978a, *ApJ*, 224, 453
 ———. 1978b, *ApJ*, 224, 857
 Herbst, W., Racine, R., & Warner, J. W. 1978, *ApJ*, 223, 471
 Hildebrand, R. H. 1988, *Astrophys. Lett.*, 26, 263
 Jones, T. J. 1990, *AJ*, 99, 1894
 Jura, M. 1980, *ApJ*, 235, 63
 Kilkenny, D., Whittet, D. C. B., Davies, J. K., Evans, A., Bode, M. F., Robson, E. I., & Banfield, R. M. 1985, *South Africa Astron. Obs. Circ.*, 9, 55
 Leitherer, C., Hefele, H., Stahl, O., & Wolf, B. 1982, *A&A*, 108, 102
 Martin, P. G. 1974, *ApJ*, 187, 461
 ———. 1989, in *IAU Symp. 135, Interstellar Dust*, ed. L. J. Allamandola & A. G. G. M. Tielens (Dordrecht: Kluwer), 55
 Martin, P. G., et al. 1992, *ApJ*, submitted
 Martin, P. G., & Whittet, D. C. B. 1990, *ApJ*, 357, 113
 Mathis, J. S. 1986, *ApJ*, 308, 281
 Moffat, A. F. J. 1971, *A&A*, 13, 30
 Muzzio, J. C. 1979, *AJ*, 84, 639
 Muzzio, J. C., & Orsatti, A. M. 1977, *AJ*, 82, 345
 Nagata, T. 1990, *ApJ*, 348, L13
 Serkowski, K. 1965, *ApJ*, 141, 1340
 ———. 1973, in *IAU Symp. 52, Interstellar Dust and Related Topics*, ed. J. M. Greenberg & D. S. Hayes (Dordrecht: Reidel), 145
 Serkowski, K., Mathewson, D. S., & Ford, V. L. 1975, *ApJ*, 196, 261
 Stephenson, C. B., & Sanduleak, N. 1971, *Publ. Warner & Swasey Obs.*, 1, No. 1
 Straizys, V., Cernis, K., & Hayes, D. S. 1985, *Ap&SS*, 112, 251
 Straizys, V., & Mesitas, E. 1980, *Acta Astron.*, 30, 541
 Strom, K. M., Strom, S. E., Carrasco, L., & Vrba, F. J. 1975, *ApJ*, 196, 489
 Strom, S. E., Vrba, F. J., & Strom, K. M. 1976, *AJ*, 81, 314
 Tanaka, M., Sato, S., Nagata, T., & Yamamoto, T. 1990, *ApJ*, 352, 724
 Ungerer, V., Mauron, N., Brillet, J., & Nguyen-Quang-Rieu, 1985, *A&A*, 146, 123
 Vrba, F. J., Coyne, G. V., & Tapia, S. 1981, *ApJ*, 243, 489
 Vrba, F. J., & Rydgren, A. E. 1984, *ApJ*, 283, 123
 ———. 1985, *AJ*, 90, 1490
 Vrba, F. J., Strom, K. M., Strom, S. E., & Grasdalen, G. L. 1975, *ApJ*, 197, 77
 Wardle, J. F. C., & Kronberg, P. P. 1974, *ApJ*, 194, 249
 Whittet, D. C. B. 1974, *MNRAS*, 168, 371
 Whittet, D. C. B., Adamson, A. J., Duley, W. W., Geballe, T. R., & McFadzean, A. D. 1989, *MNRAS*, 241, 707
 Whittet, D. C. B., Bode, M. F., Longmore, A. J., Adamson, A. J., McFadzean, A. D., Aitken, D. K., & Roche, P. F. 1988, *MNRAS*, 233, 321
 Whittet, D. C. B., Kirrane, T. M., Kilkenny, D., Oates, A. P., Watson, F. G., & King, D. J. 1987, *MNRAS*, 224, 497
 Whittet, D. C. B., & van Breda, I. G. 1978, *A&A*, 66, 57
 Wilking, B. A., & Lada, C. J. 1983, *ApJ*, 274, 698
 Wilking, B. A., Lebofsky, M. J., Martin, P. G., Rieke, G. H., & Kemp, J. C. 1980, *ApJ*, 235, 905
 Wilking, B. A., Lebofsky, M. J., & Rieke, G. H. 1982, *AJ*, 87, 695